

THANK YOU FOR YOUR ORDER

Thank you for your recent purchase from Infotrieve. If you need further assistance, please contact Infotrieve Customer Service at customerservice@infotrieve.com. Please include the Infotrieve Order ID, so we can better assist you.

This is not an invoice.

CUSTOMER INFORMATION	ORDER INFORMATION
Ordered For:	Infotrieve Order ID:
Company:	Ordered For:
Client ID:	Ordered For Email:
Address:	Ordered:
	Deliver Via:
	Delivery Address:
Country:	Tracking Info.:
Phone:	
Fax:	
Email:	
DOCUMENT INFORMATION	
Std. Num.:	Type:
Publication:	Copies:
Publisher:	Urgency:
Vol(Iss) Pg:	Genre:
Date	Total Fee:
Title:	
Author(s):	
· ,	
Usage:	
The contents of the attached document are copyrighted works. You purpose:	ou have secured permission to use this document for the following
you may have with the copyright owner or an authorized licensing has placed additional terms and conditions on your use of this doct	ther purpose but may have other rights pursuant to other arrangements body. To the extent that a publisher or other appropriate rights-holder ument, such terms and conditions are specified herein under "Copyright of the content, please purchase the appropriate permission via
Copyright Terms:	

Email: customerservice@infotrieve.com

FISEVIER

Contents lists available at ScienceDirect

Chemical Physics Letters

journal homepage: www.elsevier.com/locate/cplett



QCPMG using adiabatic pulses for faster acquisition of ultra-wideline NMR spectra

Luke A. O'Dell. Robert W. Schurko *

Department of Chemistry and Biochemistry, University of Windsor, 401 Sunset Avenue, Windsor Ontario, Canada N9B 3P4

ARTICLE INFO

Article history: Received 10 July 2008 In final form 26 August 2008 Available online 2 September 2008

ABSTRACT

A previously reported quadrupolar spin–echo experiment using adiabatic pulses, which can achieve uniform excitation of quadrupolar nuclei across a wide bandwidth, has been extended to a QCPMG-like sequence exhibiting the same uniform, broadband excitation as the echo experiment but with the advantage of a significant increase in S/N. This WURST–QCPMG sequence is used to obtain static wideline ⁷¹Ga (spin-3/2) and ⁹¹Zr (spin-5/2) spectra with linewidths in excess of 500 kHz, on a standard probe at 9.4 T without any transmitter frequency or field adjustment. The sequence is also used to observe the ⁵⁹Co (spin-7/2) central transition and inner satellite transitions.

© 2008 Elsevier B.V. All rights reserved.

1. Introduction

Static nuclear magnetic resonance (NMR) spectra of quadrupolar nuclei (nuclear spin I > 1/2) are generally more difficult to obtain in the solid state than in solution due to line-broadening caused by the anisotropic quadrupolar interaction, *i.e.*, the coupling of the non-spherical electric charge distribution of the nucleus with the surrounding electric field gradient (EFG). For half-integer spin quadrupolar nuclei in asymmetric environments (*i.e.*, sites with non-zero EFGs), this interaction can result in powder patterns with breadths of several MHz. In such cases, it is often only the central $1/2 \leftrightarrow -1/2$ transition (CT) that can be observed, being unaffected by the quadrupolar interaction to first-order. In many cases, second-order broadening is enough to spread the CT itself into the MHz regime.

Much effort has been devoted to reducing the CT linewidths of such nuclei, and significant progress has been made in this area. The development of stronger magnetic field (B_0) strengths has been crucial since the CT linewidth scales inversely with B_0 ; however, many nuclei exhibit CT linewidths in the MHz regime even at fields above 20 T. Magic angle spinning (MAS) is a commonly employed mechanical method which partially averages the second-order quadrupolar interaction by modulating the orientation of the EFG tensor relative to B_0 , although very high spinning speeds are often required for complete averaging. Fully isotropic spectra may be obtained by complete averaging of the quadrupolar interaction using more complex mechanical manipulations (DOR or DAS), or spin manipulations (MQMAS or STMAS), though each of these techniques have associated disadvantages and limitations [1]. Whilst such developments have proven immensely useful in improving spectral resolution, the static CT lineshape remains the most direct way of measuring the chemical shielding tensor and its relative

orientation to the EFG for a powder sample (single-crystal NMR is advantageous if such a crystal is available). Broad static spectra may also be sensitive to nuclear dynamics and can be used as probes of atomic/molecular exchange [2]. Ultra-wideline NMR ($ca. \ge 250 \, \text{kHz}$ width) of half-integer quadrupolar nuclei therefore remains an important technique for materials characterization, and several methods exist to overcome the difficulties associated with obtaining accurate spectral lineshapes.

For the relatively simple case of a sample featuring a single site (*i.e.*, where spectral overlap is not an issue), two main problems arise in ultra-wideline NMR. First, the dispersion of the signal intensity in the frequency domain means that extensive signal averaging may be required to obtain an acceptable signal-to-noise ratio (S/N), especially for nuclei of low gyromagnetic ratio or low natural abundance. The second crucial problem is achieving uniform excitation of the full linewidth. Standard radio frequency (rf) pulses exhibit an excitation bandwidth determined by their length, and an ultra-short rf pulse required to excite a wide bandwidth will often require very high powers to produce a significant nutation angle, often beyond the limits of standard hardware. Short rf pulses may also deviate from the ideal rectangular amplitude profile.

The problem of sensitivity can be dealt with by increasing B_0 , reducing the sample temperature or using signal enhancement procedures. The polarization of the CT can be increased by saturation/inversion of the satellite transitions (STs) using amplitude and/or phase modulated pulse sequences such as RAPT, DFS or adiabatic pulses [3]. Such methods can increase the CT signal by a factor of up to 2I, thereby dramatically reducing the overall experiment time. Another commonly used signal enhancement sequence known as Quadrupolar Carr-Purcell-Meiboom-Gill (QCPMG) [4–6] exploits the difference in T_2 (the transverse relaxation time) and T_2^* (the magnetization dephasing time) using a train of refocusing pulses, enabling the acquisition of the spin-echo multiple times in each scan. Fourier transformation of the

^{*} Corresponding author. Fax: +1 519 973 7098. E-mail address: rschurko@uwindsor.ca (R.W. Schurko).

train gives a series of narrow 'spikelets' whose manifold reproduces the frequency-domain NMR lineshape.

To compensate for the limited excitation bandwidth of rf pulses. field-sweeping involves acquiring the spectrum in a piecewise fashion with constant transmitter frequency and variation of B_0 , similar to original continuous-wave NMR methods [7-9]. The NMR signal is recorded at certain intervals and the lineshape can thus be constructed by plotting the signal intensities across a range of offset frequencies. Analogous to this method is frequency-stepping, where B_0 remains constant, the transmitter frequency itself is adjusted, and the spectrum is reconstructed either by plotting the signal intensity as a function of transmitter offset [10-13], or by co-adding each Fourier transformed sub-spectrum [14–16]. In the latter case, the size of the frequency step must be chosen to produce a net excitation profile that is uniform across the linewidth [15,16]. These techniques can easily be combined with the signal enhancement methods mentioned above. In particular, frequency-stepped QCPMG has been successfully used to obtain accurate CT lineshapes from quadrupolar nuclei such as ⁶⁷Zn [17], ⁹¹Zr [18], ²⁷Al [19] and ¹³⁹La [20] as well as spectra of spin-1/2 nuclei such as ¹⁹⁹Hg and ²⁰⁷Pb [21,22], which exhibit powder patterns broadened by chemical shift anisotropy. Wideline spectra may also be reconstructed using indirect detection methods in the presence of strong coupling to more amenable nuclei [23.24].

Aside from the obvious inefficiency of only partial excitation of the lineshape, another drawback of the frequency-stepped techniques is that with standard equipment the experimenter must be present to adjust the field/frequency between each acquisition, as well as optimizing the tuning and matching conditions of the probe, making the experiment time-consuming in terms of personnel as well as equipment. Recently, two methods have been proposed that allow the full excitation of wideline spectra without any field or transmitter frequency adjustment. Microcoils [25,26] are becoming increasingly applied in solid-state NMR (both static [27,28] and MAS [29,30]) and are capable of delivering rf powers well into the MHz regime. Short $\pi/2$ pulses may be produced which yield excitation bandwidths wide enough to cover the full CT. and even the STs in favourable cases. Although only small quantities of sample may be used (typically a few mg), the increase in inherent coil sensitivity gained by reducing the coil diameter counteracts this problem somewhat, and in many instances limited sample availability makes the use of microcoils highly advantageous to maximize the coil filling-factor.

Whereas microcoils allow for a 'brute-force' excitation of the full spectrum using high rf field strengths, the second of the newly proposed methods utilizes a more subtle approach and relatively low rf powers. Adiabatic pulses [31,32] are commonly used in magnetic resonance imaging and solution NMR to achieve broadband excitation or inversion of magnetization. They consist of amplitude- and frequency-modulated pulses which create a net magnetic field B_{eff} within the sample that, in a frequency-modulated frame rotating at the instantaneous frequency of the pulse, sweeps slowly from an orientation parallel to the external field into the transverse plane (half-passage), or to an orientation anti-parallel to the external field (full-passage). Provided that the adiabatic condition [33] is met, the nuclear magnetization will continue to precess around $B_{\rm eff}$ during the pulse, thereby following it (this mechanism is described in detail elsewhere [31,32]). Adiabatic pulses therefore allow a much wider region of magnetization to be excited/inverted than regular rf pulses. Adiabatic WURST (wideband uniform-rate smooth truncation [34]) and hyperbolic secant pulses have been finding increasing use in solid-state NMR as methods of CT signal enhancement by ST inversion or saturation [3]. In 1989, Bodenhausen and co-workers demonstrated that adiabatic pulses can be used to produce a spin-echo provided that the sweep rate of the refocusing pulse, R_{ref} , is double that of the excitation pulse, $R_{\rm exc}$ [35]. Very recently, Bhattacharyya and Frydman successfully applied this pulse sequence to wideline NMR of half-integer spin quadrupolar nuclei and also examined the frequency-dispersed echoes that occur upon departing from the $R_{\rm ref}$ = $2R_{\rm exc}$ condition, whose magnitudes resemble the shape of the frequency-domain lineshape, allowing the frequency-domain spectrum to be obtained without the need for Fourier transformation [36]. The authors showed that such methods produced accurate lineshapes with significant gains in S/N over standard spin–echo sequences.

Herein we present an extension of this adiabatic echo sequence to a QCPMG-like version that combines the broadband excitation of adiabatic pulses with the signal enhancement advantage of QCPMG. Practical implementation of the sequence is described in Section 2 and advantages and limitations are discussed in the Results and Summary sections. Elsewhere, we will present an application of solenoidal microcoils to wideline NMR and a comparison of the technique in terms of sensitivity with both frequency-stepping and adiabatic spin-echoes [37].

2. Experimental details

The WURST-QCPMG sequence is shown in Fig. 1. The sequence is a modification of the frequency-swept echo pulse sequence (N = 1) introduced by Bhattacharyya and Frydman [36] (hereafter referred to as the WURST-echo sequence) with a Meiboom-Gill loop placed around the refocusing pulse and acquisition period, analogous to the regular QCPMG experiment [4]. Delays τ_2 and τ_3 are included in the repeating loop to allow the rf circuitry time to switch between transmission and acquisition modes. WURST A is an excitation pulse whose frequency is swept adiabatically between positive and negative offset frequencies at a constant rate, $R_{\rm exc}$. These offsets do not necessarily have to be equal, but the spectra herein were obtained with a symmetric excitation pulse swept from +f to -f (see Table 1 for values of f). WURST B is a refocusing π -pulse, R_{ref} , again swept at a constant rate between positive and negative offsets. The WURST-QCPMG spectra reported herein were obtained with the refocusing pulses swept between +f and -f, i.e., the same sweep range as the excitation pulse. WURST-80 pulse shapes were used in all cases [34], but in principle other frequency-swept adiabatic pulse shapes may be used in the same way. P_1 and P_2 were both set to 50 µs, rendering the sweep rates $R_{\rm exc}$ and $R_{\rm ref}$ identical and therefore yielding frequency-dispersed echoes. Eight-step phase cycling was employed as in Ref. [36], and each spectrum was acquired twice, with opposite frequencysweep directions in the second experiment. The two spectra were then co-added to compensate for lineshape distortion due to the occurrence of transverse relaxation over the duration of the frequency-dispersed echoes [36]. WURST-echo experiments were also performed under the $R_{\rm ref}$ = $2R_{\rm exc}$ condition, with a 50 μs WURST A excitation pulse swept from +f to -f and a 50 μ s WURST B refocusing pulse swept from +2f to -2f.

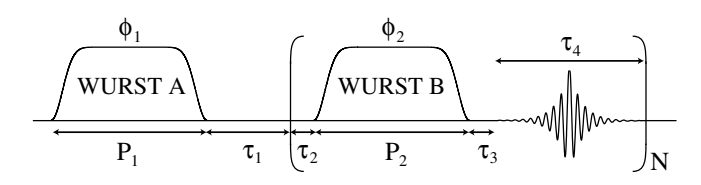


Fig. 1. The WURST–QCPMG pulse sequence. WURST A and B are frequency-swept adiabatic pulses [34] used for excitation and refocusing of transverse magnetisation, respectively. N=1 corresponds to the echo sequence of Bhattacharyya and Frydman [36]. An eight-step nested phase cycle was used ($\varphi_1 = \varphi_{\text{receiver}} = 0$, $\pi/2$, π , $3\pi/2$, $\varphi_2 = \varphi_1 + \pi/2$, $\varphi_1 - \pi/2$).

Table 1
Experimental parameters used for the WURST-echo and WURST-QCPMG experiments

Nucleus	Spin	Larmor frequency at 9.4 T (MHz)	Sample	Sample mass (g)	Pulse sequence	Offset f (kHz)	Sweep rate (MHz ms ⁻¹)	τ ₁ (μs)	τ ₂ (μs)	τ ₃ (μs)	τ ₄ (μs)	N	v _{exc} (kHz)	v _{ref} (kHz)	Dwell time (µs)	Number of scans
⁸⁷ Rb	3/2	130.79	Rb ₂ SO ₄	0.153	WURST-echo WURST-QCPMG WURST-QCPMG	50 50 50	R _{exc} = 2 2 2	1000 976 476	3 3 3	10 10 10	256 2000 1000	1 50 120	3.0 2.7 2.7	6.6 2.7 2.7	1.0 10.0 10.0	2048 2048 512
⁷¹ Ga	3/2	121.85	GaPcCl	0.057	WURST-echo WURST-QCPMG	350 400	$R_{\text{exc}} = 14$ 16	50 16	3	10 10	256 80	1 80	14.3 12.3	29.6 12.3	1.0 1.0	32 000 24 000
⁹¹ Zr	5/2	37.07	ZrO ₂ NMR rotor	1.316	WURST-echo WURST-QCPMG	350 400	$R_{\text{exc}} = 14$ 16	50 26	3	14 10	256 100	1 100	25.0 20.6	31.0 20.6	1.0 1.0	40 000 20 000
⁵⁹ Co	7/2	96.02	Co(acac) ₃	0.061	WURST-QCPMG	1000	40	26	3	10	100	100	6.0	6.0	0.5	80000

The sweep rate was identical for both pulses in the WURST-QCPMG experiment, and $R_{\text{ref}} = 2R_{\text{exc}}$ for the echo experiment. Powers were determined experimentally by visual inspection of the spectral lineshape. The number of scans in the final column represents the sum of two experiments of opposite sweep direction.

As detailed by Bhattacharyya and Frydman, the pulse lengths and the inter-pulse delay determine the position of the spin-echo in τ_4 (or the 'mid-point' of a frequency-dispersed echo if $R_{\rm ref} \neq 2R_{\rm exc}$, where 'mid-point' here refers to the part of the echo arising from crystallites resonating at the transmitter frequency) [36]. In order to obtain a series of narrow, uniformly-shaped spikelets in the frequency domain after Fourier transformation, it is crucial that the echoes acquired are uniformly-spaced and have the same phase in the time domain. For the parameters and phase-cycling employed herein, this required careful setting of the parameter τ_1 to the values given in Table 1. It is possible that the pulse sequence may be improved to eliminate such a restriction on the echo delay, and we are currently working to achieve this. As with the regular QCPMG experiment, the spikelet separation in the frequency domain is the inverse of the echo separation in the time domain, and is thus equal to τ_4^{-1} .

The optimum pulse powers for the WURST-echo and WURST-QCPMG sequences were determined experimentally by visual inspection of the Fourier transformed spectrum, using Bhattacharyya and Frydman's expressions $v_{\rm exc}\approx 0.25R_{\rm exc}^{1/2}(I+1/2)^{-1}$ and $v_{\rm ref}\approx 0.8R_{\rm ref}^{1/2}(I+1/2)^{-1}$ as initial values, where the units of R are kHz/ms [36]. In practise, the most accurate spectral lineshapes for the WURST-QCPMG experiments reported here were obtained using powers $v_{\rm exc}=v_{\rm ref}=A\cdot R^{1/2}(I+1/2)^{-1}$, with A ranging from 0.12 to 0.49 (see Table 1). In general, lower powers resulted in accurate lineshapes but loss of signal intensity, whereas higher powers resulted in severe lineshape distortion.

The WURST-QCPMG sequence detailed above was tested on a series of quadrupolar nuclei of various half-integer spin values at 9.4 T using a commercial 4.0 mm triple-resonance MAS probe and a Varian InfinityPlus spectrometer. 50 µs WURST pulse lengths and a 0.5 s recycle delay were used in all cases. Exponential line broadening was applied to all WURST-QCPMG spectra (20 Hz for the ⁸⁷Rb spectra and 200 Hz for all others) and a magnitude function was applied after Fourier transformation to obtain absorptive spikelets. Full details of the other experimental parameters used are given in Table 1. The samples of rubidium sulphate (Rb₂SO₄), gallium phthalocyanine chloride (GaPcCl) and cobalt(III) acetylacetonate (Co(acac)₃) were obtained from Sigma Aldrich or Alfa Aesar and used without further purification. For the 91Zr experiment, an empty zirconia 4.0 mm o.d. Varian MAS NMR rotor was used. 87Rb spectra were referenced against 1.0 M aqueous RbNO₃, ⁷¹Ga against 1.0 M aqueous Ga(NO₃)₃, ⁹¹Zr against a saturated solution of Cp₂ZrCl₂ in CH₂Cl₂ and ⁵⁹Co against aqueous 1.0 M K₃Co(CN)₆, with all solution resonances set to 0 ppm. Spectral simulations were generated using Dmfit [38]. The WURST-QCPMG pulse sequence is available upon request.

3. Results and discussion

3.1. 87Rb of Rb₂SO₄

At 9.4 T the ⁸⁷Rb NMR spectrum of Rb₂SO₄ covers a width of *ca*. 35 kHz, which is narrow enough to be fully excited using regular rf pulses. However, short, low-power pulses must be used to avoid differences in nutation rates for the two rubidium sites, which differ significantly in their C_0 (quadrupolar coupling constant) values. Fig. 2a shows the ⁸⁷Rb spectrum obtained using the WURST-echo sequence and 2b and c are high- and low-resolution WURST-QCPMG spectra, respectively. All spectra are shown with correct relative amplitudes. Accurate lineshapes were obtained using both sequences, closely matching the simulation in Fig. 2d. Rubidium sulphate features two distinct rubidium sites of equal abundance whose NMR parameters have previously been determined via single-crystal NMR [39]. Parameters obtained from our fit were $\delta_{\rm iso} = 42 \pm 1$ ppm, $C_{\rm O} = 2.8 \pm 0.1$ MHz and $\eta_{\rm O} = 0.95 \pm 0.05$ for site 1, and $\delta_{\rm iso} = 15 \pm 1$ ppm, $C_{\rm O} = 5.7 \pm 0.2$ MHz and $\eta_{\rm O} = 0.15 \pm 0.05$ for site 2, in close agreement with the established values. An iterative fit of the two discontinuities on the low-field side of the site 2 lineshape in the WURST-echo spectrum resulted in rough estimates of the chemical shift anisotropy (CSA) parameters Ω = 84 ± 30 ppm and κ = -0.95 ± 0.30, with Euler angles α = 65°, β = 10° and γ = 110° (all ±40°), which despite giving an excellent fit, agree to a lesser extent with values previously reported [39]. More accurate CSA parameters would likely be obtained by repeating the experiment at a higher field.

The gain in signal obtained by using WURST-OCPMG over the WURST-echo sequence is clear from Fig. 2. The values given on the right hand side of each spectrum (in this and subsequent figures) are the relative maximum signal amplitudes, adjusted for the number of scans acquired. As with the regular QCPMG experiment, the exact increase in S/N depends on the spikelet separation, which can be seen by comparing Fig. 2b and c. The choice of spikelet separation is a compromise between signal enhancement factor and spectral resolution. The higher resolution WURST-QCPMG experiment resulted in approximately five times as much signal as the WURST-echo while still accurately reproducing the spectral lineshape. It should be remembered that the WURST-echo pulse sequence has already been shown to give a gain in S/N over lowpower, short-pulse echo experiments [36], so the enhancement due to the WURST-QCPMG experiment over such echo experiments is considerable. The relatively low sweep rate suggests that shorter pulse lengths could be used to obtain even higher signal gains, although how short the WURST pulses can go will be limited by the power of the pulse (shorter pulses require faster sweep rates

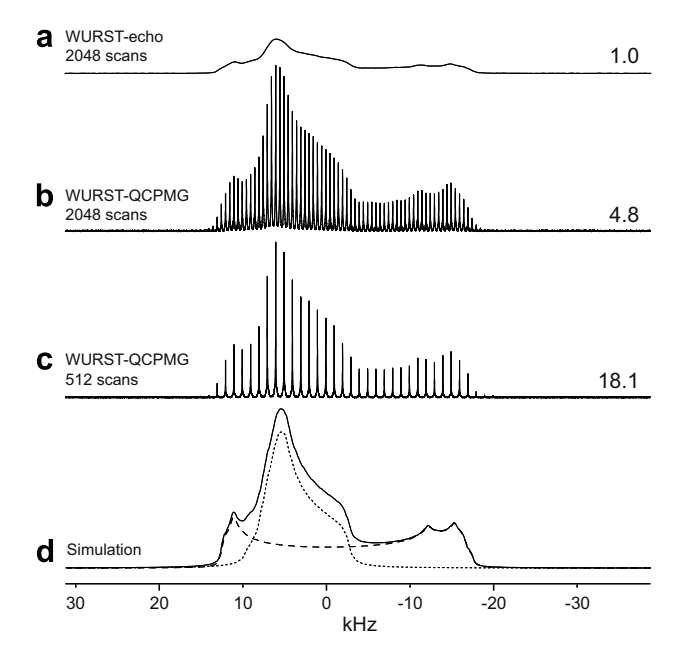


Fig. 2. 87 Rb NMR spectra of Rb₂SO₄ obtained using (a) the WURST–echo and (b) and (c) the WURST–QCPMG sequence. A simulation of the spectrum is shown in (d), with the separate lines shown for site 1 (dotted) and site 2 (dashed). Values on the right (in this and subsequent figures) are the maximum relative signal amplitudes corrected for the number of scans acquired.

to retain their adiabaticity, and therefore need higher rf field strengths) and the pulse programmer resolution of the spectrometer.

The relative intensities of the signals from the two rubidium sites were $52.4 \pm 3\%$ for site 1 and $47.6 \pm 3\%$ for site 2, in excellent agreement with the 1:1 ratio of the structure. This is a demonstration of the ability of adiabatic spin–echo sequences like WURST–echo and WURST–QCPMG to produce quantitative spectra from half-integer quadrupolar nuclei.

3.2. 71Ga of GaPcCl

As a more challenging test of the applicability of these pulse sequences to ultra-wideline NMR, 71Ga spectra were obtained from a sample of gallium phthalocyanine chloride, the crystal structure of which features a single gallium site [40], giving rise to a static ⁷¹Ga CT lineshape of ca. 500 kHz in breadth at 9.4 T. As can be seen in Fig. 3, the full width of this line was successfully excited using an offset value f = 350-400 kHz. Offsets smaller than this produced severe distortion of the lineshape. The WURST-QCPMG experiment successfully reproduced the same lineshape as the WURST-echo experiment, with a gain in signal of 3.6. The ⁷¹Ga simulation was generated by an analytical fit of spectra obtained at 9.4 and 21.1 T, yielding parameters $\delta_{\rm iso}$ = 130 ppm, $C_{\rm Q}$ = 21.2 MHz, $\eta_{\rm Q}$ = 0.05, Ω = 150 ppm, κ = 0.8, α = 50°, β = 15° and γ = 10°. A combined experimental and computational study of this compound, as well as related structures, will be the subject of a future publication. Overall, the lineshape reflects the simulation reasonably well, with even the central discontinuity at ca. 0 kHz visible in the WURST-QCPMG spectrum. However, some minor lineshape distortion is visible on the low-frequency side of the lineshape, which could potentially be eliminated using more selective phase cycling [41]. A 16-step phase cycle identical to that given in Ref. [5] for the original QCPMG experiment was tested and produced an identical lineshape but with the signal intensity reduced by 50%. Investigation of other phase cycling schemes is underway.

3.3. 91Zr of a ZrO₂ MAS NMR rotor

Several zirconia polymorphs were characterized using wideline static 91Zr NMR in 1992 by Bastow and Smith [42] using the frequency-stepped technique, and more recently a 91Zr NMR spectrum of a 5.0 mm o.d. zirconia MAS NMR rotor was obtained using frequency-stepped QCPMG [18]. While producing reliable lineshapes and allowing the extraction of NMR parameters and quantification of the different zirconia phases, these spectra were time-consuming to acquire due to the reasons outlined in the introduction (ca. 9 h per spectrum in the former work, ca. 6 h in the latter). Fig. 4 is a clear illustration of the advantage of the WURST-OCPMG experiment over WURST-echo sequence in acquiring such spectra, with the spectrum in Fig. 4b obtained in under 3 h without any frequency adjustment. As in Ref. [18], the spectrum can be accurately simulated with two lines (Fig. 4c), one arising from tetragonal ZrO₂ (δ_{iso} = 60 ± 50 ppm, C_Q = 19.6 ± 0.2 MHz, $\eta_0 = 0.0 \pm 0.1$) and a second from the orthorhombic phase $(\delta_{\rm iso} = 240 \pm 50 \text{ ppm}, C_{\rm Q} = 18.3 \pm 0.3 \text{ MHz}, \eta_{\rm Q} = 0.95 \pm 0.1)$. The ratio of the tetragonal to orthorhombic phase is determined as 0.9:1, a slightly higher ratio than the 0.7:1 reported in Ref. [18]. Despite the ⁹¹Zr linewidth being comparable in width to the ⁷¹Ga spectrum above, significantly more rf power was required for the WURST pulses, which is likely due to the low gyromagnetic ratio of the ⁹1Zr nucleus.

3.4. ⁵⁹Co of Co(acac)₃

Fig. 5 demonstrates that the WURST–QCPMG experiment is by no means limited to the central transition and that satellite transitions may also be excited using frequency-swept adiabatic pulses. ⁵⁹Co is a spin-7/2 nucleus and thus has seven single-quantum Zeeman transitions. As mentioned in the introduction, CT lineshapes tend to be much narrower than the STs since the CT is only affected by the quadrupolar interaction to second order. First order quadru-

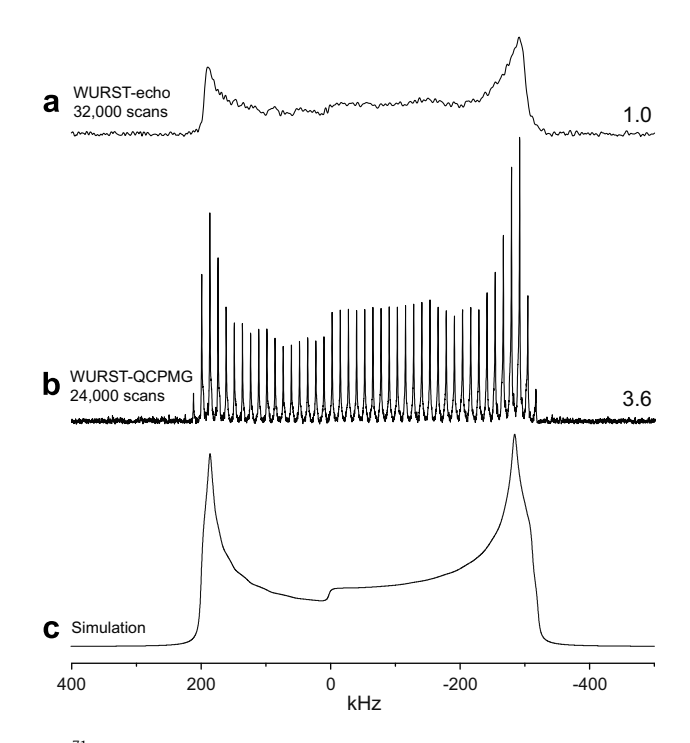


Fig. 3. 71 Ga NMR spectra of gallium phthalocyanine chloride obtained using (a) the WURST-echo and (b) the WURST-QCPMG sequence. A simulation of the lineshape, based on multiple-field data, is shown in (c).

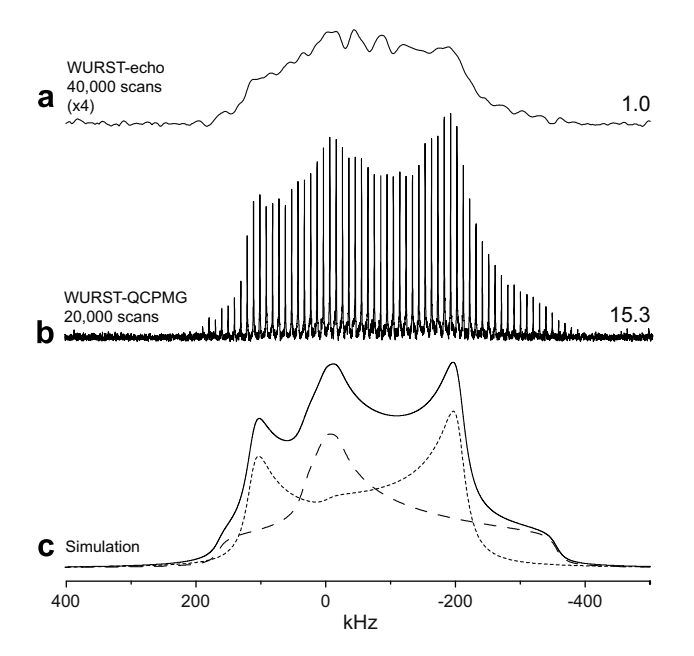


Fig. 4. ⁹¹Zr spectra obtained from a ZrO₂ MAS NMR rotor using (a) the WURST–echo sequence (vertical scale multiplied by four) and (b) the WURST–QCPMG sequence. A simulation of the spectrum is shown in (c), with lineshapes arising from the tetragonal (dotted) and orthorhombic (dashed) zirconia phases.

polar broadening spreads the ⁵⁹Co ST signals from the single cobalt site in Co(acac)₃ across a range of ca. 1.4 MHz at 9.4 T (see the simulation in Fig. 5a, generated using parameters δ_{iso} = 12500 ppm, $C_0 = 5.5 \text{ MHz}, \ \eta_0 = 0.2, \ \Omega = 1190 \text{ ppm}, \ \kappa = -0.57, \ \alpha = 75^{\circ}, \ \beta = 86^{\circ}$ and $\gamma = 15^{\circ}$, reported previously [43]). Using a significantly wider offset value than in the other experiments described above (see Table 1), a large portion of the STs was excited and observed using the WURST-OCPMG pulse sequence (Fig. 5b). The discontinuities on the inner STs ($\pm 3/2 \leftrightarrow \pm 1/2$) are visible in the spectrum and their positions line up reasonably well with those of the simulation. Partial excitation of the $\pm 5/2 \leftrightarrow \pm 3/2$ STs can also be seen in the figure. A WURST-echo spectrum was not attempted on this sample. The optimum rf powers required were relatively low given the fast sweep rate used, which is probably due to the high spin number of ⁵⁹Co. It is likely that the full ST manifold could be acquired by frequency-stepping the WURST-QCPMG experiment, which should also remove the need for sweeping the frequency in both directions. This is currently under investigation.

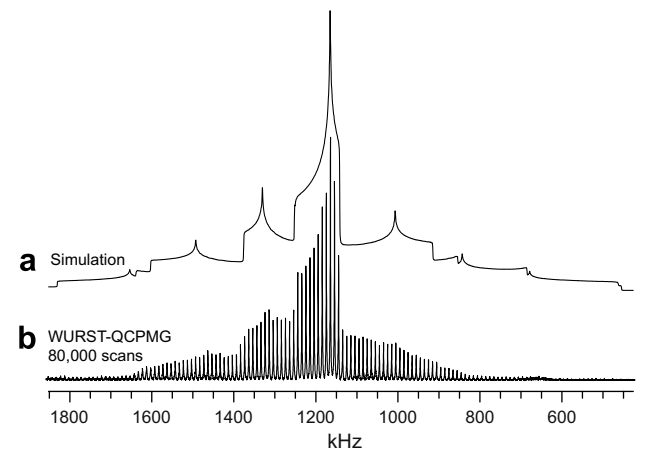


Fig. 5. ⁵⁹Co simulation (a) and WURST-QCPMG spectrum (b) of Co(acac)₃.

4. Summary

Bhattacharvva and Frydman's WURST-echo experiment, which can achieve uniform and quantitative excitation of quadrupolar nuclei across a wide bandwidth [36], has been extended to a QCPMG-like sequence that exhibits the same uniform, broadband excitation as the WURST-echo experiment but with the advantage of a significant increase in S/N. A simple variation on the general sequence shown in Fig. 1, using a WURST-80 excitation pulse swept between +f and -f at constant rate R, a WURST-80 refocusing pulse identical in length and sweep range, and an eight-step phase cycle, has been used to produce a train of equidistant frequency-dispersed echoes. As with the regular QCPMG experiment, this echo train can be Fourier transformed into a spikelet spectrum that accurately reflects the true spectral lineshape. Optimum powers for the WURST pulses were determined experimentally and found to be $v_{\text{exc}} = v_{\text{ref}} = A \cdot R^{1/2} (I + \frac{1}{2})^{-1}$, where A ranged from 0.12 to 0.49. Relative to the fairly amenable spin-3/2 nucleus ⁷¹Ga, higher rf powers were necessary for the low- γ 91Zr experiment and lower powers were required for the high spin number ⁵⁹Co nucleus. Since the optimum powers for the WURST pulses depend primarily on the sweep rate R and spin number I, this experiment is independent of C_0 and is therefore relatively straightforward to optimize for a new sample once a sufficient excitation bandwidth has been established. The minimum required offset value f was found to be approximately 30% beyond the edge of the lineshape under observation. All spectra were acquired twice, with the frequency direction reversed in the second experiment, and subsequently co-added to compensate for T_2 relaxation across the length of the frequency-dispersed echoes. The sequence is shown to produce a significant gain in S/N over the WURST-echo sequence, and can offer far shorter experimental times than frequency-stepped techniques for wideline NMR. A quantitative comparison of the sensitivity of the sequence with that of frequency-stepping and microcoil methods will be reported elsewhere [37].

The main limitation of the WURST–QCPMG pulse sequence is determined by the adiabaticity limit of the pulses. For relatively narrow spectra, short pulses and fast sweep rates may be used, with the maximum sweep rate limited by the pulse programmer resolution of the spectrometer. In order to retain adiabaticity for wider spectra (*i.e.*, larger offset values) while keeping pulse lengths reasonably short, the rf powers must be increased, and due to the significant fraction of scan time spent pulsing, the duty factor will increase rapidly. Longer pulse lengths are an alternative to increasing the power, but potential signal will then be lost due to transverse relaxation. Optimum powers for the WURST pulses were found to decrease with increasing gyromagnetic ratio, and also for higher spin numbers (*e.g.*, 5/2, 7/2), and the sequence therefore should become more efficient in these cases.

The general WURST-QCPMG pulse sequence presented herein shows much potential for optimization. More selective phase cycling could prove to be advantageous and other adiabatic pulse shapes may be used for the excitation and refocusing pulses. Signal enhancement techniques such as RAPT, DFS or adiabatic inversion of STs may also be incorporated onto the front end of the pulse sequence when only the CT signal is of interest, providing further signal enhancement. Further development of the sequence and applications to spin-1/2 nuclei are currently underway.

Acknowledgements

Professor Lucio Frydman and Dr. Rangeet Bhattacharyya are gratefully acknowledged for providing the WURST-echo pulse sequence. The Natural Sciences and Engineering Research Council

(NSERC, Canada), the Canadian Foundation for Innovation and the Ontario Innovation Trust are acknowledged for financial support. RWS thanks the Ontario Ministry of Research and Innovation for an Early Researcher Award, and acknowledges the Centre for Catalysis and Materials Research at the University of Windsor for additional funding. LAO thanks Foreign Affairs and International Trade Canada (DFAIT) for a Government of Canada Post-Doctoral Research Fellowship. Joel A. Tang is thanked for help with the simulations and useful discussions.

References

- [1] K.J.D. MacKenzie, M.E. Smith, Multinuclear Solid-State NMR of Inorganic Materials, Pergamon, 2002.
- [2] R.W. Schurko, S. Wi, L. Frydman, J. Phys. Chem. B 106 (2002) 51.
- [3] R. Siegel, T.T. Nakashima, R.E. Wasylishen, Concepts Magn. Reson. A 26 (2005)
- [4] S. Bank, J.F. Bank, P.D. Ellis, J. Phys. Chem. 93 (1998) 4847.
- [5] F.H. Larsen, H.J. Jakobsen, P.D. Ellis, N.C. Nielsen, J. Phys. Chem. A 101 (1997) 8597.
- [6] R. Siegel, T.T. Nakashima, R.E. Wasylishen, Concepts Magn. Reson. A 26 (2005) 62.
- [7] H.E. Rhodes, P.K. Wang, H.T. Stokes, C.P. Slichter, J.H. Sinfelt, Phys. Rev. B 26 (1982) 3559.
- [8] X. Wu, E.A. Juban, L.G. Butler, Chem. Phys. Lett. 221 (1994) 65.
- [9] I.J.F. Poplett, M.E. Smith, Solid State Nucl. Magn. Reson. 11 (1998) 211.
- [10] D.W. Sindorf, V.J. Bartuska, J. Magn. Reson. 85 (1989) 581.
- [11] M.A. Kennedy, R.L. Vold, R.R. Vold, J. Magn. Reson. 192 (1991) 320.
- [12] T.J. Bastow, M.E. Smith, S.N. Stuart, Chem. Phys. Lett. 191 (1992) 125.
- [13] P.L. Bryant et al., J. Am. Chem. Soc. 123 (2001) 12009.
- [14] S.W. Sparks, P.D. Ellis, J. Am. Chem. Soc. 108 (1986) 3215.

- [15] D. Massiot, I. Farnan, N. Gautier, D. Trumeau, A. Trokiner, J.P. Coutures, Solid State Nucl. Magn. Reson. 4 (1995) 241.
- [16] A. Medek, V. Frydman, L. Frydman, J. Phys. Chem. A 103 (1999) 4830.
- [17] A.S. Lipton, G.W. Buchko, J.A. Sears, M.A. Kennedy, P.D. Ellis, J. Am. Chem. Soc. 123 (2001) 992.
- [18] I. Hung, R.W. Schurko, J. Phys. Chem. B 108 (2004) 9060.
- [19] J.A. Tang, J.D. Masuda, T.J. Boyle, R.W. Schurko, Chem. Phys. Chem. 7 (2006) 117.
- [20] H. Hamaed, A.Y.H. Lo, D.S. Lee, W.J. Evans, R.W. Schurko, J. Am. Chem. Soc. 128 (2006) 12638.
- [21] I. Hung, A.J. Rossini, R.W. Schurko, J. Phys. Chem. A 108 (2004) 7112.
- [22] R. Siegel, T.T. Nakashima, R.E. Wasylishen, J. Phys. Chem. B 108 (2004) 2218.
- [23] C.P. Grey, A.J. Vega, J. Am. Chem. Soc. 117 (1995) 8232.
- [24] Z. Gan, Chem. Commun. (2008) 868.
- [25] K.R. Minard, R.A. Wind, Concepts Magn. Reson. 13 (2001) 128.
- [26] K.R. Minard, R.A. Wind, Concepts Magn. Reson. 13 (2001) 190.
- [27] K. Yamauchi, J.W.G. Janssen, A.P.M. Kentgens, J. Magn. Reson. 164 (2004) 87.
- [28] A.P.M. Kentgens et al., J. Chem. Phys. 128 (2008) 052202.
- [29] J.W.G. Janssen, A. Brinkmann, E.R.H. van Eck, J.M. van Bentum, A.P.M. Kentgens, J. Am. Chem. Soc. 128 (2006) 8722.
- [30] D. Sakellariou, G. Le Goff, J.F. Jacquinot, Nature 447 (2007) 694.
- [31] M. Garwood, L. DelaBarre, J. Magn. Reson. 153 (2001) 155.
- [32] A. Tannús, M. Garwood, NMR Biomed. 10 (1997) 423.
- [33] E. Kupče, R. Freeman, J. Magn. Reson. A 117 (1995) 246.
- [34] Ē. Kupče, R. Freeman, J. Magn. Reson. A 115 (1995) 273.
- [35] J.-M. Bohlen, M. Rey, G. Bodenhausen, J. Magn. Reson. 84 (1989) 191.
- [36] R. Bhattacharyya, L. Frydman, J. Chem. Phys. 127 (2007) 194503.
- [37] J.A. Tang, L.A. O'Dell, P.M. Aguiar, B.E.G. Lucier, D. Sakellariou, R.W. Schurko, in preparation.
- [38] D. Massiot et al., Magn. Reson. Chem. 40 (2002) 70.
- [39] T. Vosegaard, J. Skibsted, H. Bildsøe, H.J. Jakobsen, J. Magn. Reson. A 122 (1996)
- [40] J.P. Linsky, T.R. Paul, R.S. Nohr, M.E. Kenney, Inorg. Chem. 19 (1980) 3131.
- [41] P.R. Bodart, J.P. Amoureux, Y. Dumazy, R. Lefort, Mol. Phys. 98 (2000) 1545.
- [42] T.J. Bastow, M.E. Smith, Solid State Nucl. Magn. Reson. 1 (1992) 165.
- [43] C.W. Kirby, W.P. Power, Can. J. Chem. 79 (2001) 296.